

# Sonochemical Reaction to Control the Near Infrared Photoluminescence Properties of Single-Walled Carbon Nanotubes

Yutaka Maeda,<sup>a\*</sup> Yui Konno,<sup>a</sup> Akane Nishino,<sup>a</sup> Michio Yamada,<sup>a</sup> Saki Okudaira,<sup>b</sup> Yuhei Miyauchi,<sup>b</sup> Kazunari Matsuda,<sup>b</sup> Jun Matsui,<sup>c</sup> Masaya Mitsuishi<sup>d</sup>, and Mitsuaki Suzuki<sup>e</sup>

<sup>a</sup> Department of Chemistry, Tokyo Gakugei University, Tokyo 184-8501, Japan

<sup>b</sup> Institute of Advanced Energy, Kyoto University, Uji, Kyoto 611-0011, Japan

<sup>c</sup> Department of Material and Biological Chemistry, Yamagata University, Yamagata 990-8560, Japan

<sup>d</sup> Institute of Multidisciplinary Research for Advanced Materials (IMRAM), Tohoku University, Sendai 980-8577, Japan

<sup>e</sup> Department of Chemistry, Josai University, Sakata, Saitama 350-0295, Japan

## Abstract

The effect of ultrasonic irradiation on the optical properties of single-walled carbon nanotubes (SWNTs) was investigated. Upon sonication in D<sub>2</sub>O in the presence of sodium dodecylbenzene sulfate (SDBS) under air, red-shifted photoluminescence (PL) peaks at ~1043 and ~1118 nm were observed from aqueous suspensions of (6,4) and (6,5)SWNTs, accompanied by a decrease in the intensity of the intrinsic PL peaks. Upon sonication with SDBS under Ar atmosphere, the rate of spectral change increased with the sonication time and new PL peaks emerged at 1043, 1118, and 1221 nm. Meanwhile, upon the addition of 1-butanol, PL peaks emerged only at 1043 nm and 1118 nm, while the emergence of that at 1221 nm was inhibited. On the other hand, a suspension with highly dispersed SWNTs was obtained upon sonication in the presence of sodium cholate without any change in the intrinsic optical properties of SWNTs. These experimental results reveal that the PL characteristics of SWNTs can be controlled by controlling the sonication conditions such as the type of surfactant used, the concentration of SWNTs, reaction environment, and the presence of an inhibitor such as 1-butanol.

## 1. Introduction

Since their discovery, single-walled carbon nanotubes (SWNTs) have attracted special attention because of their outstanding mechanical strength and unique electrical and optical properties based on

their band structures.<sup>1-2</sup> The structures of SWNTs are distinguished by a chiral index (n,m), which is defined using the vectors of the graphene sheet.<sup>3</sup> The chiral index can be assigned experimentally through optical analysis such as absorption, photoluminescence (PL), or Raman spectral analysis.<sup>4-6</sup> The PL of SWNTs in the near-infrared (NIR) region has been studied actively for applications in imaging, sensing, and optoelectronics because biological tissues are highly transparent to NIR light and the PL wavelength lies in the telecommunication window.<sup>7-9</sup> Observation of the PL of SWNTs requires excitation with secondary transition ( $E_{22}$ ) energies because of the small Stokes shift of the first transition ( $E_{11}$ ) energy. Recently, sidewall functionalization of SWNTs has been utilized to control the local band structure, and in particular, to obtain a new red-shifted NIR PL peak with high efficiency.<sup>10-18</sup> This allows for excitation with the  $E_{11}$  energy to observe the emission of functionalized SWNTs in the NIR region, resulting in their improved performance as photoluminescent materials in bioimaging applications. It is important to precisely control the degree of functionalization because the PL efficiencies of functionalized SWNTs depend on their degree of functionalization.<sup>19-21</sup> For the measurement of the PL of SWNTs, low-concentration suspensions with individually dispersed SWNTs is preferred, because PL quenching occurs at high concentrations owing to the interaction with other chiral SWNTs. In pioneering studies reported by Weisman and co-workers, highly dispersed SWNTs were prepared in a D<sub>2</sub>O solution containing sodium dodecyl sulfate (SDS) by a sonication and centrifugation process to study their PL properties.<sup>22</sup> Although sonication and centrifugation of SWNTs is a valid approach to prepare individually dispersed SWNTs, it is also known to damage and shorten SWNTs.<sup>23-25</sup>

From the viewpoint of environmental issues, sonochemical degradation of surfactants has been investigated to remove the surfactants. It has been reported that the degradation of the surfactant proceeds *via* the generation of radical species.<sup>26-28</sup> Generally, SWNTs are known to be highly reactive to radical species.<sup>29-30</sup> Here, we developed a simple, convenient, and effective approach to control the PL properties of SWNTs through ultrasonic irradiation with an appropriate surfactant under the optimized conditions of the irradiation time, SWNT concentration, and reaction atmosphere.

## 2. Experimental

### General

The (6,5)-enriched SWNTs (SG 65i) used in this work were purchased from Sigma-Aldrich. Reagent-grade sodium cholate (SC), SDS, and sodium dodecylbenzene sulfonate (SDBS) were purchased from commercial suppliers. Optical absorption spectra were recorded on a UV-vis-NIR spectrophotometer (V-670; Jasco Corp.) with a Pyrex cell with a 10-mm path length. Raman spectra of SWNT samples were acquired after the filtration of the samples with 514.5, 561, and 633 nm excitation using a Raman spectrophotometer (LabRAM HR-800; Horiba Ltd.). The obtained spectra were normalized relative to

the G band. Photoluminescence spectra were obtained using a spectrophotometer equipped with a 450-W lamp and a Symphony-II CCD detector (Nanolog; Horiba Ltd.). The excitation and emission wavelengths were varied from 500–1000 nm and 827–1600 nm, respectively. The excitation and the emission slit widths were 10 nm, respectively. The PL intensity was corrected to the data correction time of each sample.

For sample preparation, ultrasonic irradiation in a bath sonicator (B2510J-MT ultrasonic cleaner; Branson) was used. The suspension of SWNTs was centrifuged at 140,000 g for 1 h in a high-speed centrifuge equipped with a P70AT2 angle rotor (CP80 $\beta$ ; Hitachi Koki Co., Ltd.) or a S58A angle rotor (Micro ultracentrifuge CS100FNX; Hitachi Koki Co., Ltd.). For PL measurement, an adequate dose of the D<sub>2</sub>O solution containing a surfactant was added to the suspension depending on the concentration. After sonication, the resulting suspension was centrifuged for 1 h at 140,000 g. X-ray photoelectron spectroscopy (XPS) was conducted using an X-ray photoelectron spectrometer (PH 5600; PerkinElmer) with a Mg *K* $\alpha$  X-ray source.

Up-conversion PL (UCPL) spectroscopy was performed using a Si-based CCD cooled with liquid nitrogen (Princeton Instruments, SPEC-10). A 1064 nm laser with a power density of 2175 W/cm<sup>2</sup> was used as the excitation light source for recording the UCPL spectra. The spectra were recorded with samples placed in a quartz cell at room temperature using multiple optical filters to eliminate the direct reflection/scattering of the excitation light from the quartz cell and samples.

#### Typical procedure A

SWNTs (0.25 mg) and 20 mL of a D<sub>2</sub>O solution of the surfactant (1 wt%) were added to a 50 mL screw bottle. The suspension was treated for 30 min by ultrasonic irradiation in a bath sonicator. Then, the suspension was divided into 4 mL fractions in 50 mL screw bottles, and was sonicated for 0.5 to 5.5 h (the total sonication time is 1 h to 6 h), respectively. The suspension was at 140,000g for 1 h at 15 °C. Then, 80% of the supernatant was recovered and filtered with cotton. The concentration of SWNTs was adjusted using its absorbance at the local minimum near 775 nm by the addition of D<sub>2</sub>O containing 1 wt% surfactant. After 10 min of sonication, the suspension was centrifuged at 140,000g for 1 h at 15 °C, and 80% of the supernatant was recovered and filtered with cotton.

#### Typical procedure B

D<sub>2</sub>O was purged with Ar by bubbling Ar for 30 min. SWNTs (0.4 mg), SDBS (447 mg, 1.3 mmol), and Ar-purged D<sub>2</sub>O (40 mL) were added to an Ar-purged 50 mL two-necked flask. The suspension was sonicated for 30 min to 10 h by ultrasound irradiation in a bath sonicator. Sampling of the suspension (4 mL) was conducted using a syringe at 30 min, 1 h, 1.5 h, 2 h, 4 h, 6 h, 8 h, and 10 h. The suspensions obtained after sampling were centrifuged at 140,000g for 1 h at 15 °C. Then, 80% of the supernatant was recovered and filtered with cotton. The concentration of SWNTs was adjusted using its absorbance at the local minimum near 775 nm by the addition of D<sub>2</sub>O containing 1 wt% SDBS. After 10 min of sonication, the suspension was centrifuged at 140,000g for 1 h

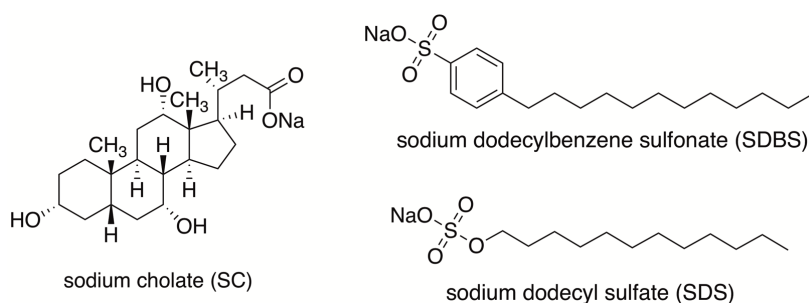
at 15 °C and 80% of the supernatant was recovered and filtered with cotton. The sonication experiment under oxygen was conducted according to the same procedure using oxygen instead of Ar. In the experiments in the presence of 1-butanol, 0.4 mL of 1-butanol was added to the two-necked flask before sonication.

### 3. RESULTS AND DISCUSSION

In this study, SC, SDS, and SDBS were selected as typical surfactants to disperse SWNTs in D<sub>2</sub>O (Chart 1). Typically, 0.25 mg of SWNTs in 20 mL of D<sub>2</sub>O containing 1 wt% of one of the surfactants was sonicated for 1–6 h (see Procedure A, Experimental section). After sonication, ultracentrifugation was conducted at 140,000g for 1 h to obtain a supernatant containing well-dispersed SWNTs. Characteristic absorption and PL peaks assigned to SWNTs were observed from the supernatant obtained using SC and no significant spectral changes were observed with the variation in the sonication time from 1 h to 6 h (Figure 1 and S1a). On the other hand, the characteristic absorption and PL peak intensities of the supernatant prepared using SDS were low compared to that observed for the supernatant obtained using SC as the surfactant (Figure 2 and S1b). In addition, the intensity of the characteristic peaks in absorption and PL spectra decreased with increasing sonication time. The  $E_{11}$  absorption peaks at 875 and 980 nm and PL peaks at ~876 and ~979 nm with decreased intensities are assigned to (6,4) and (6,5)SWNTs, respectively. When SDBS was used as a surfactant to disperse the SWNTs, the SWNT dispersibility was found to be as good as that obtained with SC, which indicates that SDBS is effective for dispersing SWNTs well (Figure S1b). This result is consistent with the results reported by Resasco and co-workers.<sup>31</sup> In addition, in the presence of SDBS, a decrease in the intensity of the intrinsic absorption and PL peaks assigned to (6,4) and (6,5)SWNTs was observed after 6 h of sonication, accompanied by the emergence of red-shifted PL peaks at 1043 and 1118 nm (Figure 3).

The excitation spectra corresponding to the red-shifted PL peaks at 1043 and 1118 nm showed peak maximum at 581 and 872 nm and 567 and 973 nm, respectively (Figure 4). As the features of the excitation spectra are in good agreement with the features of the absorption spectra of (6,4) and (6,5)SWNTs, the red-shifted PL peaks at ~1043 and ~1118 nm are assigned to functionalized (6,4) and (6,5)SWNTs, respectively. The positions of the PL peaks also agree well with those observed previously from oxidized (6,4) and (6,5)SWNTs (1050 and 1120 nm).<sup>10-12</sup>

**Chart 1.** Chemical structures of surfactants



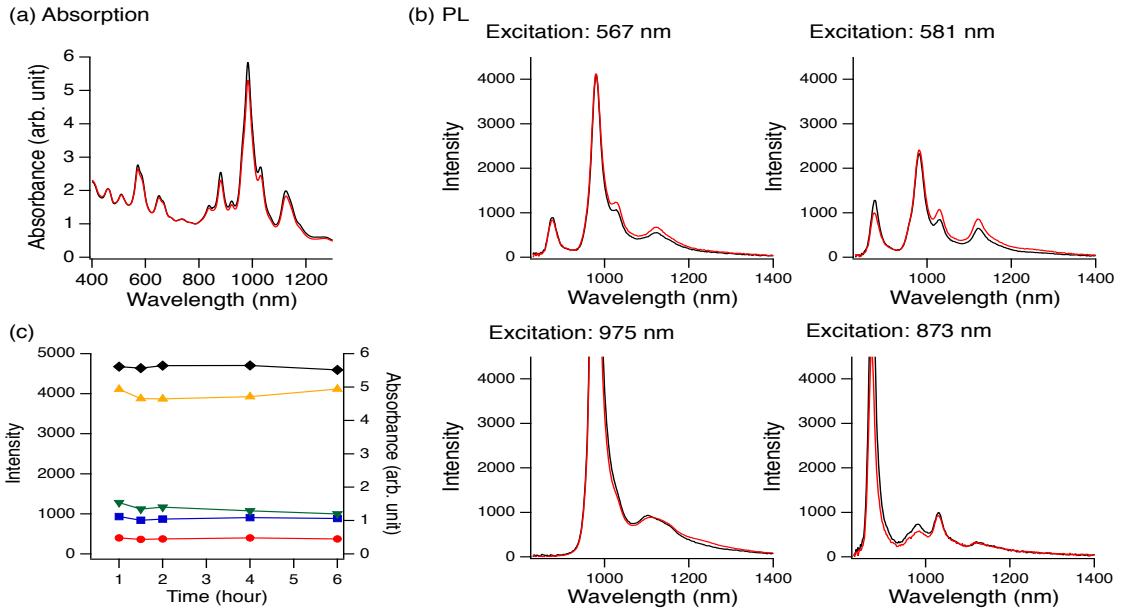


**Figure 1.** (a) Absorption spectra normalized to the local minimum near 780 nm and (b) PL spectra under excitation at 567, 581, 873, and 975 nm of SWNTs (0.0125 g/L) dispersed in a D<sub>2</sub>O solution containing 1 wt% SC. Black: 1 h of sonication, Red: 6 h of sonication. (c) Time-dependent changes in the characteristic peak intensities in (a) and (b). Black: Change in the  $E_{11}$  absorption peak intensity of (6,5)SWNTs. Yellow: Change in the PL peak at ~975 nm when excited at 567 nm. Green: Change in the PL peak at ~869 nm when excited at 581 nm. Red: Change in the PL peak at ~1048 nm when excited at 873 nm. Blue: Change in the PL peak at ~1118 nm when excited at 975 nm.

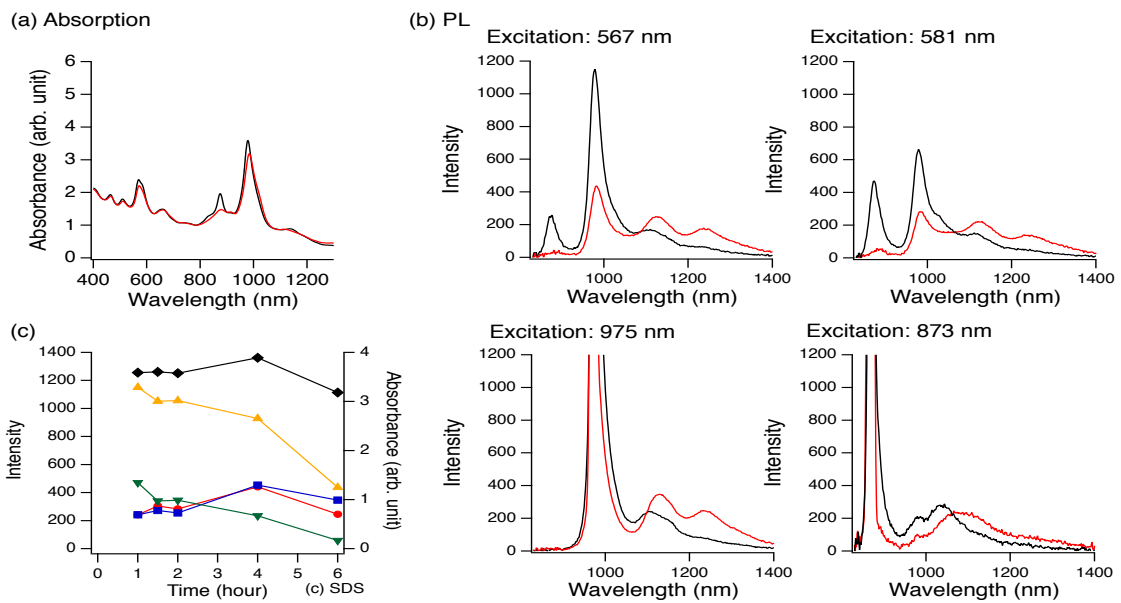


**Figure 2.** (a) Absorption spectra normalized to the local minimum near 780 nm and (b) PL spectra under excitation at 567, 581, 873, and 975 nm of SWNTs (0.0125 g/L) dispersed in a D<sub>2</sub>O solution containing 1

wt% SDS. Black: 1 h of sonication, Red: 6 h of sonication. (c) Time-dependent changes in the characteristic peak intensities in (a) and (b). Black: Change in the intensity of the  $E_{11}$  absorption peak of (6,5)SWNTs. Yellow: Change in the PL peak at  $\sim 975$  nm when excited at 567 nm. Green: Change in the PL peak at  $\sim 869$  nm when excited at 581 nm. Red: Change in the PL peak at  $\sim 1048$  nm when excited at 873 nm. Blue: Change in the PL peak at  $\sim 1118$  nm when excited at 975 nm.

To confirm the sidewall functionalization of SWNTs due to sonication, Raman spectral study was conducted. As shown in Figure 5, the ratio of the intensity of the D band to that of the G band (D/G) increased upon sonication in the presence of SDS. This result indicates that defects are introduced into SWNTs upon ultrasonic irradiation, leading to a change in the intrinsic optical properties of SWNTs. No significant change in the D/G was observed for the SWNTs sonicated in the presence of SC or SDBS under the experimental condition. As described later (Table S1), an increase in the D/G of SWNTs was observed upon using SDBS as the surfactant, depending on the sonication condition. These results suggest that SC is an effective dispersing reagent of SWNTs that does not cause a change in the intrinsic optical properties of SWNTs, while ultrasonic irradiation with SDBS is potentially effective for obtaining new red-shifted PL peaks.

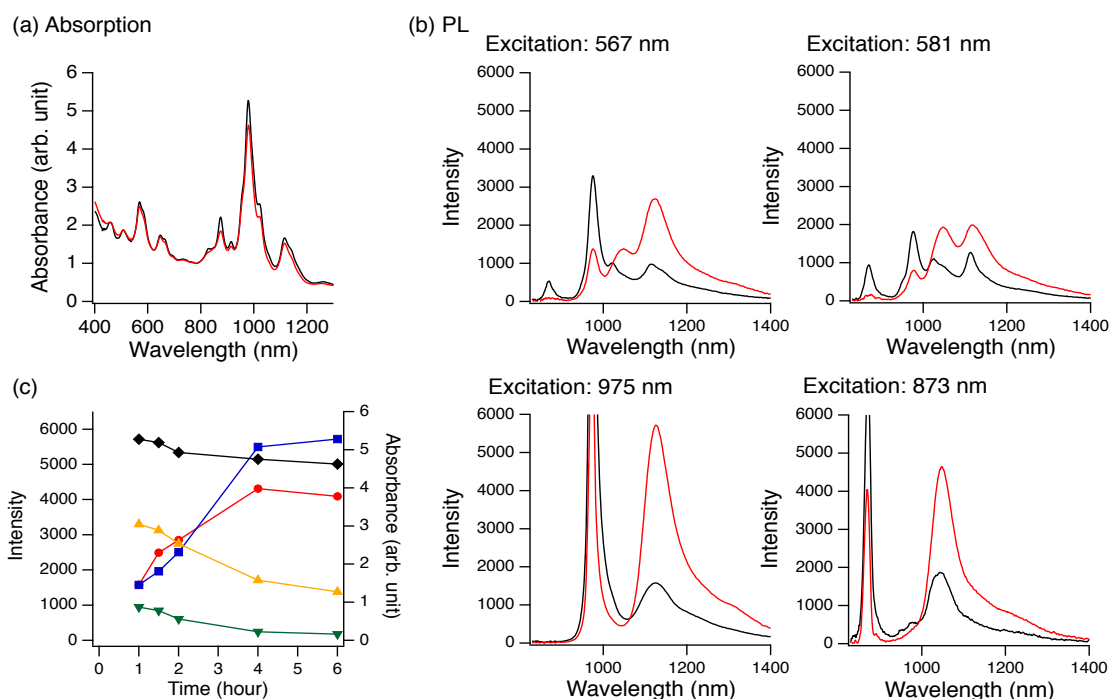


**Figure 3.** (a) Absorption spectra normalized to the local minimum near 780 nm and (b) PL spectra under excitation at 567, 581, 873, and 975 nm of SWNTs (0.0125 g/L) dispersed in a  $D_2O$  solution containing 1 wt% SDBS. Black: 1 h of sonication, Red: 6 h of sonication. (c) Time-dependent changes in the characteristic peak intensities in (a) and (b). Black: Change in the intensity of the  $E_{11}$  absorption peak of (6,5)SWNTs. Yellow: Change in the PL peak at  $\sim 975$  nm when excited at 567 nm. Green: Change in the PL peak at  $\sim 869$  nm when excited at 581 nm. Red: Change in the PL peak at  $\sim 1048$  nm when excited at 873 nm. Blue: Change in the PL peak at  $\sim 1118$  nm when excited at 975 nm.

nm when excited at 581 nm. Red: Change in the PL peak at ~1048 nm when excited at 873 nm. Blue: Change in the PL peak at ~1118 nm when excited at 975 nm.

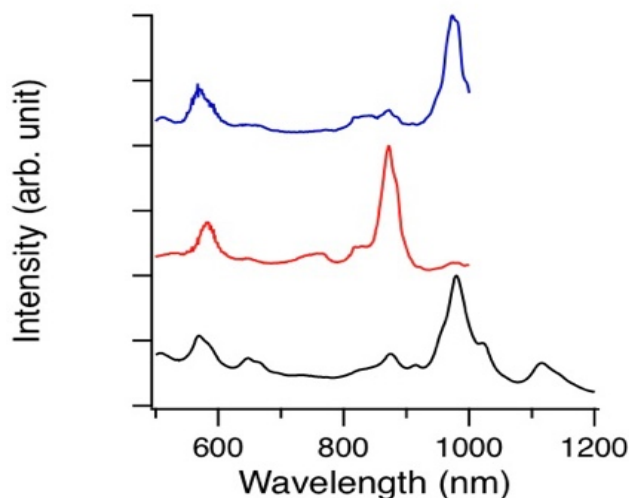


**Figure 4.** Absorption spectrum (Black) and excitation spectra (Red: 1044 nm, Blue: 1118 nm) of SWNTs (0.0125 g/L) dispersed in a D<sub>2</sub>O solution containing 1 wt% SDBS for 6 h.

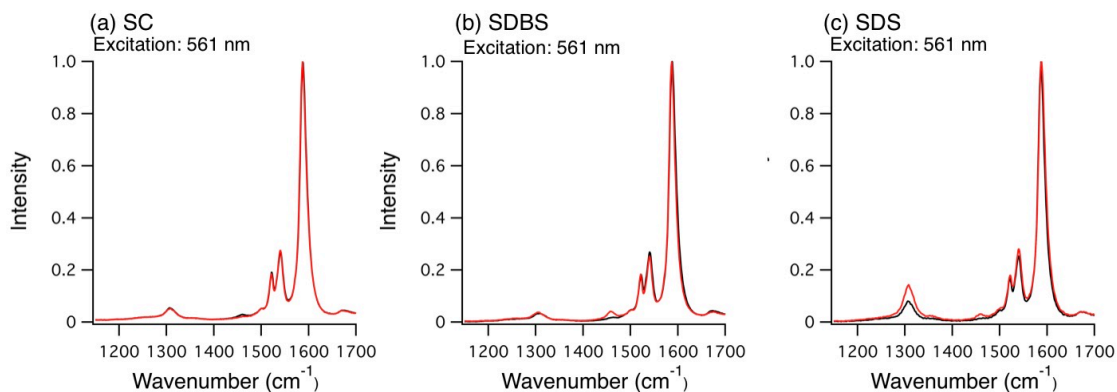


**Figure 5.** Raman spectra of SWNTs (films) after sonication in a D<sub>2</sub>O solution containing different surfactants: (a) SC, (B) SDBS, (C) SDS. Excitation wavelength is 561 nm. Sonication time: 1 h (black), 6 h (red).

To investigate the factors responsible for the emergence of the red-shifted PL peaks upon ultrasonic irradiation, firstly, we focused on studying the influence of the SWNT concentration during sonication on the PL characteristics. When the concentration of SWNTs was low (0.01 and 0.1 g/L), the red-shifted PL peaks emerged with a decrease in the intensity of the intrinsic PL peaks of SWNTs with sonication (Figure 6d and 6e). On the other hand, the red-shifted PL peaks did not emerge when the concentration of SWNTs was high (0.5 g/L) (Figure 6f). Thus, the concentration of SWNTs is an important factor in changing their intrinsic optical properties efficiently upon ultrasonic irradiation.

It has been reported that the sonochemical degradation of SDBS in water is caused by the hydroxyl radical ( $\text{OH}^\cdot$ ) generated during the sonication of  $\text{H}_2\text{O}$ .<sup>26-28</sup> The generation of radical species from a surfactant *via* hydrogen abstraction by  $\text{OH}^\cdot$  has been confirmed by electron spin resonance (ESR) spin-trapping studies.<sup>26</sup> Tour and co-workers reported the photochemical hydroxylation of SWNTs dispersed in  $\text{H}_2\text{O}$  containing SDBS under Ar atmosphere, and this reaction was suppressed in the presence of oxygen due to the radical scavenging ability of oxygen.<sup>32</sup> Kataura and co-workers reported that the treatment of SWNTs with hydrogen peroxide caused the oxidation of small-diameter (5,4)SWNTs, leading to the emergence of a red-shifted PL peak.<sup>33</sup> Based on these reported studies,  $\text{OH}^\cdot$ ,  $\text{H}_2\text{O}_2$ , and radical species generated from SDBS *via* hydrogen abstraction are considered as plausible reactive species that generate quantum defects on the SWNTs upon ultrasonic irradiation. In addition, it has been reported that the decomposition rate of organic compounds by sonication increased under Ar atmosphere than under oxygen or ambient atmosphere.<sup>34-35</sup> To confirm the influence of oxygen, the sonication of SWNTs (0.01 g/L) in an aqueous solution containing SDBS was conducted under Ar or oxygen atmosphere (See Procedure B, experimental section). Interestingly, the rate of decrease in the intensity of the  $E_{11}$  absorption and  $E_{11}$  PL peaks increased significantly under Ar atmosphere than under oxygen or ambient atmosphere (Figure 7a and S7). In addition, a new PL peak emerged at  $\sim 1221$  nm from (6,5)SWNTs after 4 h of sonication under Ar atmosphere (see excitation spectra in Figure S11). On other hand, even upon sonication for a long period of up to 46 h under air, the new PL peak at 1221 nm did not emerge (Figure S7b).

In previous studies, PL peak at 1093–1268 nm from (6,5)SWNTs has been observed after alkylation,<sup>12-14, 36-37</sup> but no peak at 1221 nm was observed from (6,5)SWNTs upon their oxidation.<sup>10-11, 38</sup> Therefore, there is a possibility that the new PL peak at 1221 nm is derived from functionalized (6,5)SWNTs that reacted with radical species generated by the sonochemical decomposition of SDBS under Ar atmosphere. In order to obtain further information, the sonication of SWNTs was conducted in the presence of 1-butanol (Procedure B), because it has been reported that the sonochemical degradation of SDBS is suppressed by the addition of an alcohol.<sup>28, 32</sup> As shown in Figure 7b, the emergence of the PL peak at 1221 nm was suppressed in the presence of 1-butanol under Ar atmosphere, while the intensity of the PL peaks at 1043 and 1118 nm increased significantly. The selective and efficient emergence of the red-shifted PL peaks indicates that a specific reaction takes place selectively in the presence of 1-butanol under Ar atmosphere. On the other hand, there was no remarkable difference in the PL wavelength regardless of the presence of 1-butanol under ambient condition (Figure 7c and S7b). These results indicate the addition of the decomposed products of SDBS generated *via* a hydrogen abstraction by  $\text{OH}^\cdot$  contributes in the emergence of the new PL at 1221 nm under Ar atmosphere.



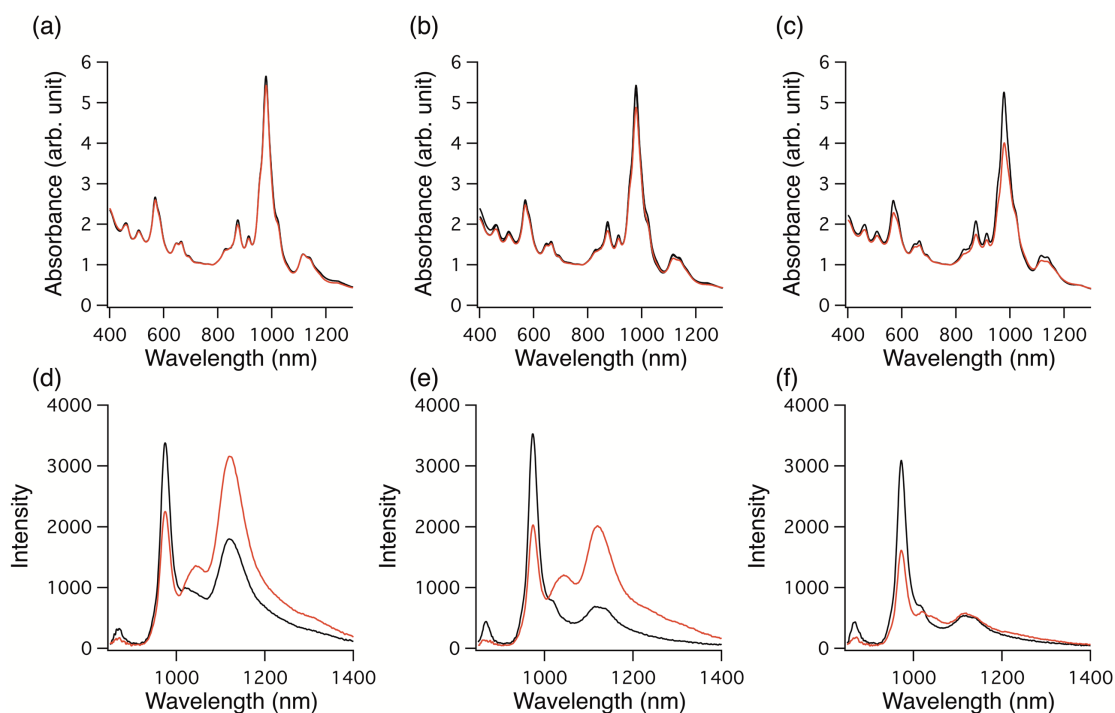


**Figure 6.** (a–c) Absorption and (d–f) PL spectra under excitation at 567 nm of SWNTs after sonication in a D<sub>2</sub>O solution containing SDBS. Concentration of SWNTs (a, d): 0.01 g/L. (b, e): 0.1 g/L. (c, f) 0.5 g/L. Sonication time: 1.5 h (black); 6 h (red).

The decomposition of SDBS in the presence of H<sub>2</sub>O<sub>2</sub> is promoted by a metal catalyst such as an Fe ion.<sup>28</sup> To confirm the influence of the metal catalyst on the sonochemical reaction, a control experiment was conducted. An SWNT suspension in a D<sub>2</sub>O solution containing SDBS (dispersion-A) was prepared by sonication for 1.5 h. A part of dispersion-A was centrifuged to remove the contaminants and obtain supernatant-1 (Figure 8, Black line). Supernatant-1 was then sonicated further for 4.5 h and then centrifuged to collect supernatant-2 (Figure 8, Blue line). The rest of dispersion-A was sonicated further for 4.5 h and then centrifuged to collect supernatant-3 (Figure 8, Red line). In comparison with the spectral features of supernatant-1, the changes in the absorption and PL spectra of supernatant-2 were smaller than those of supernatant-3, indicating that the sonochemical reaction is promoted by contaminants such as the metal catalyst. The results also indicate the contribution of OH<sup>·</sup> and/or H<sub>2</sub>O<sub>2</sub> to the emergence of red-shifted PL peaks at 1043 and 1118 nm. Thus, the purity of SWNTs is important for the preparation of SWNT suspensions by sonication when their intrinsic optical properties are to be maintained.

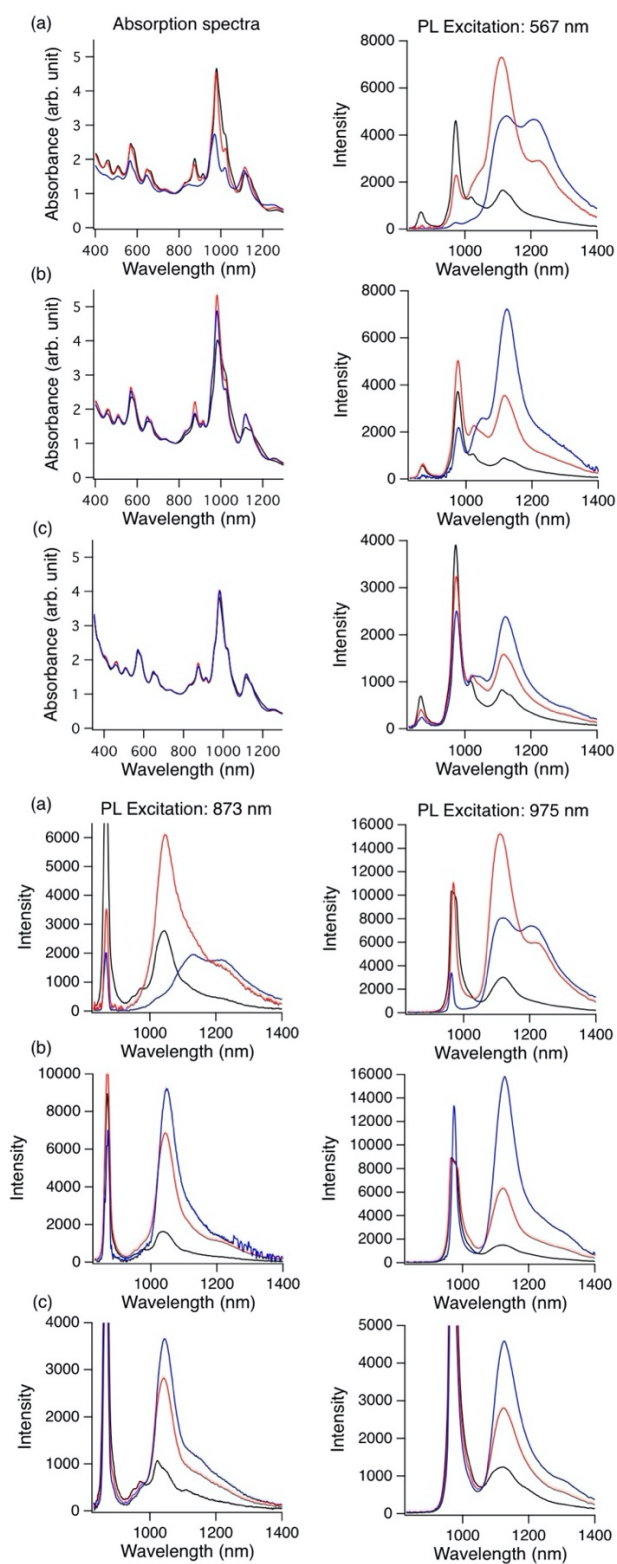


**Figure 7.** Absorption spectra and PL spectra under excitation at 567, 873, and 975 nm of SWNTs (0.01 mg/mL) dispersed in a D<sub>2</sub>O solution containing 1 wt% SDBS: (a) Ar atmosphere, (b) Ar atmosphere with 1-butanol, and (c) ambient condition with 1-butanol. Sonication time: 0.5 h (Black), 4 h (Red), 10 h (Blue).

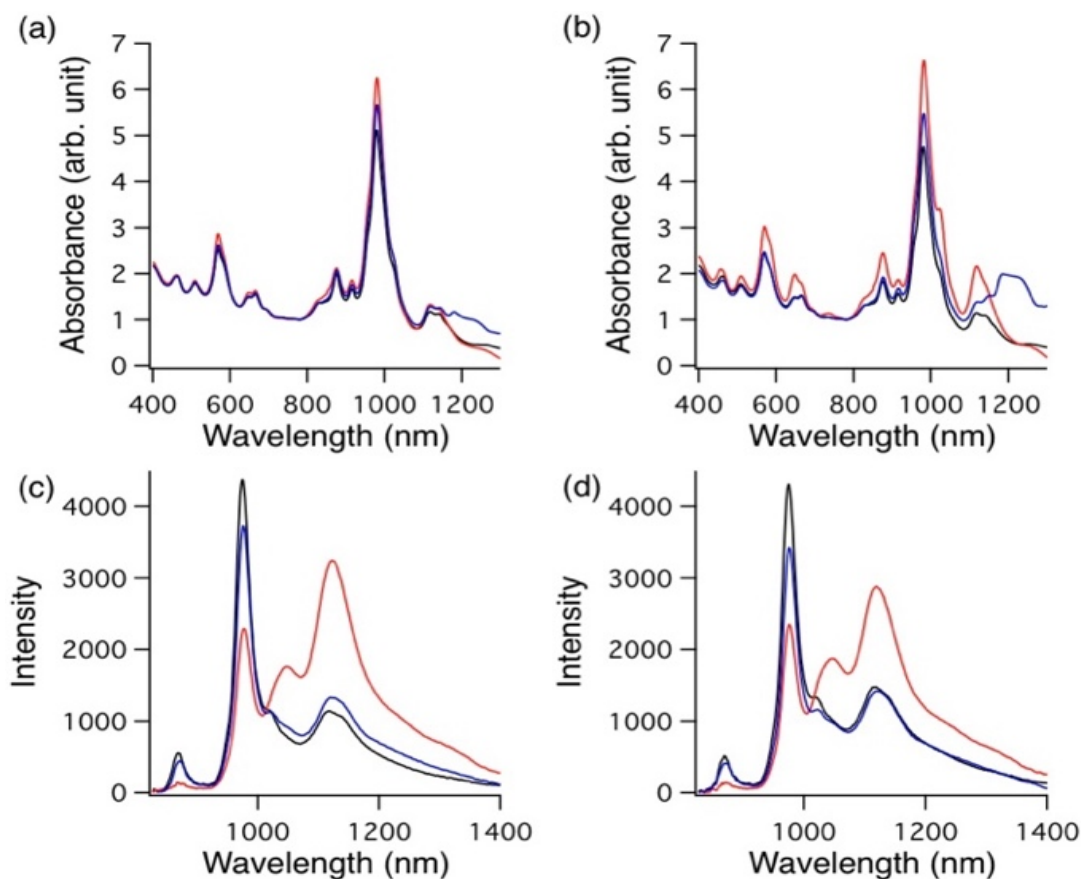


**Figure 8.** Absorption spectra (a, b) and PL spectra under 567 nm excitation (c, d) of SWNTs (a, c: 0.019 mg/mL, b, d: 0.039 mg/mL) dispersed in a D<sub>2</sub>O solution containing 1 wt% SDBS. Black: Supernatant of SWNT suspension prepared by sonication (1.5 h) and centrifugation (Supernatant-1). Blue: Supernatant of SWNT suspension prepared by sonication (1.5 h), centrifugation, and subsequent additional sonication (4.5 h) (Supernatant-2). Red: Supernatant of SWNT suspension prepared by sonication (6 h) and centrifugation (Supernatant-3).

Akizuki and co-workers reported that an intrinsic free exciton PL peak can be observed at room temperature by the excitation of SWNTs at a new mid gap state generated by chemical functionalization.<sup>39</sup> The up-conversion PL (UCPL) of SWNTs in the NIR region has attracted attention in bio-imaging owing to the low autofluorescence and phototoxicity than PL. Therefore, SWNTs (0.01 g/L) dispersed in D<sub>2</sub>O containing SDBS were excited at 1064 nm to examine the emergence of the UCPL and its dependence on the chiral structure of SWNTs. Figure 9c clearly shows UCPL peaks at ~1030, 980, 960, and 880 nm for (7,5), (6,5), (8,3), and (6,4)SWNTs at room temperature, respectively. Interestingly, the distinct UCPL peak of (6,4)SWNTs was observed at ~880 nm, although the difference between the excitation (1064 nm) and UCPL (~880 nm) wavelengths, which corresponds to the energy difference  $\Delta_{(6,4)} \sim 240$  meV, is much larger than that for other SWNTs (e.g.,  $\Delta_{(6,5)} \sim 100$  meV for

(6,5)SWNTs). Assuming a simple thermal up-conversion (detrapping) of localized excitons to free excitons in the UCPL process of SWNTs,<sup>39</sup> the exciton up-conversion rate for (6,4)SWNTs with a large  $\Delta$  should be much smaller than that for (6,5)SWNTs; the energy difference ( $\Delta_{(6,4)} - \Delta_{(6,5)} \sim 140$  meV) may result in a difference in the exciton thermal up-conversion rate at room temperature ( $T = 300$  K) approximately by a factor of  $\exp[(\Delta_{(6,4)} - \Delta_{(6,5)})/k_B T] \sim 2 \times 10^2$ , where  $k_B$  is the Boltzmann constant. Thus, considering the lower abundance of (6,4) than (6,5)SWNTs (deduced to be  $\sim 1/3$ – $1/5$  from the ratio of the absorbance peaks), the intensity of the UCPL of (6,4)SWNTs is expected to be much smaller than that of (6,5)SWNTs by a factor of  $10^{-3}$  when only the energy difference is taken into account. However, the experimental UCPL intensity ratio of (6,4) to (6,5)SWNTs is only  $\sim 1/30$ – $1/50$ , which is  $\sim 20$ – $30$  times larger than  $10^{-3}$ . This result could be attributed to the differences in the density of defect-derived local states that function as initial states of the up-conversion process, chirality-dependent electron-phonon coupling strength, and/or the resonance condition of the initially excited states (defect-derived local states) with the excitation laser wavelength (1064 nm). We verified the third mechanism from the observation of the PL excitation spectra at 1064 nm of the SWNTs, which is shown in Figure 9d. The excitation spectrum of the 1064 nm emission showed similar spectral features to that of the 1043 nm emission at which a red-shifted PL peak for functionalized (6,4)SWNTs emerged, as shown in Figure 9b. In both excitation spectra corresponding to 1064 and 1043 nm, excitation peaks at  $\sim 880$  nm coincident with the  $E_{11}$  absorption peak of (6,4)SWNTs (Figure 9a) were clearly observed. These results suggest that the local states generated in functionalized (6,4)SWNTs are near-resonant with the 1064 nm excitation light, while functionalized (6,5)SWNTs that show PL from the local states at 1118 nm (Figure 9b) are off-resonant. Therefore, the unexpectedly high UCPL intensity of functionalized (6,4)SWNTs under the 1064 nm excitation is partially attributed to the resonant excitation of the initial state. From a practical viewpoint, the result suggests that the functionalized (6,4)SWNTs will be useful for UCPL imaging applications, because they provide UCPL at a wavelength shorter than 900 nm at which conventional silicon-based detectors have much higher sensitivity than for the UCPL of (6,5)SWNTs at 980 nm.

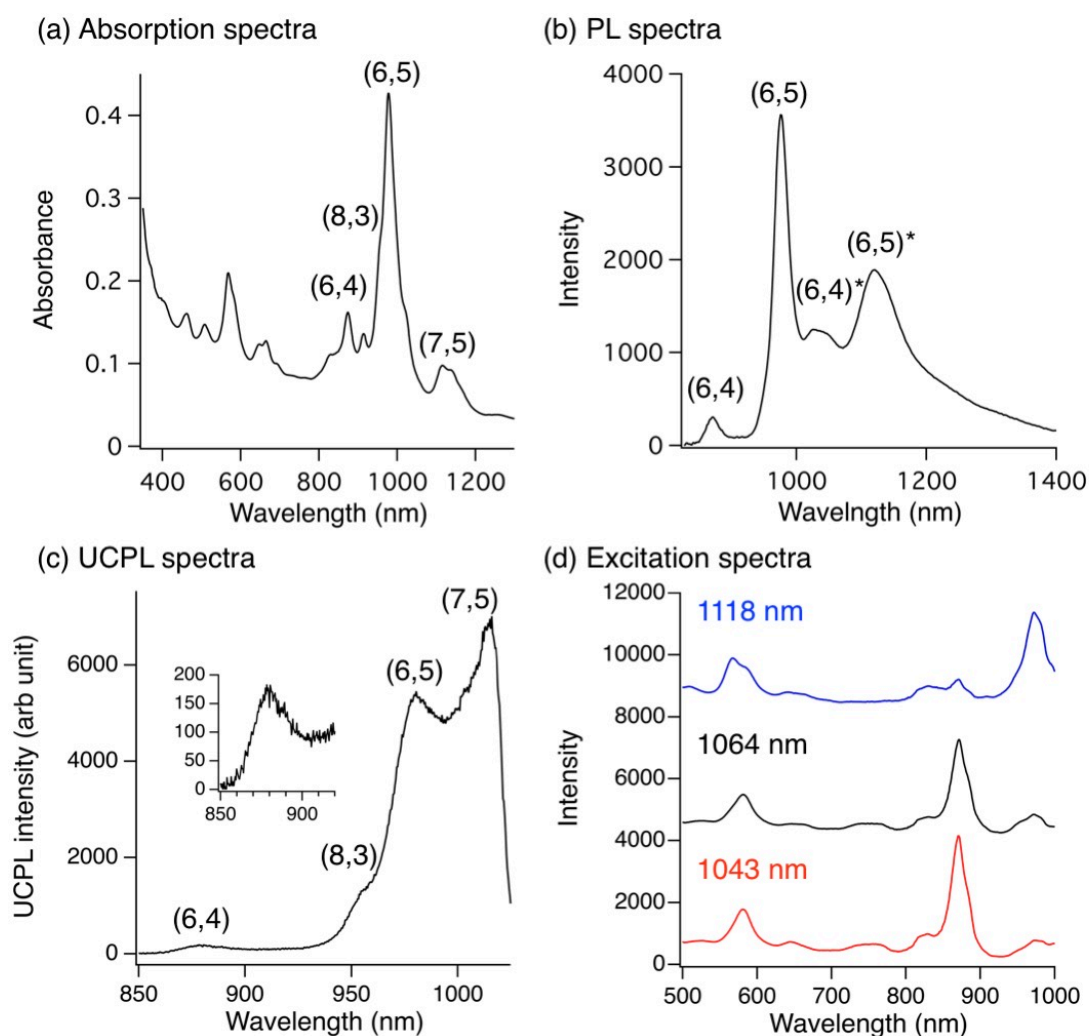


**Figure 9.** Absorption (a), PL (excitation wavelength: 567 nm) (b), UCPL (c), and PL excitation (red: 1043 nm, black: 1064 nm, blue: 1118 nm) (d) spectra of SWNTs dispersed in D<sub>2</sub>O containing 1 wt% SDBS. Sample preparation: 0.1 mg of SWNTs was dispersed in 10 mL of D<sub>2</sub>O containing 1 wt% SDBS for 2 h under ambient condition, and then centrifuged at 140,000 g for 1 h.

The elemental analysis of the resultant SWNT samples was performed by XPS. XPS peaks assignable to carbon and oxygen groups were observed as dominant peaks at ~285 and 532 eV, respectively (Figure S12). The atomic percentages of oxygen groups for the SWNTs sonicated for a short time in the presence of SDBS were found to be relatively high, suggesting that the oxidation of SWNTs occurred under sonication (Table S1, Entry 3, 6, 10, and 12). However, the relative atomic percentages of oxygen groups over carbon groups decreased with an increase in the sonication time, regardless of the change in D/G of the Raman spectra (Table S1; Entry 7-9, 11, 13, and 15). It has been reported that upon the heat treatment of oxidized SWNTs, the decomposition reaction is more likely to proceed than the elimination reaction as the amount of oxygen atoms increases.<sup>20, 40-41</sup> The mismatch in the Raman D/G

and the atomic percentage of oxygen over carbon observed XPS might be due to the competition between the oxidation of SWNTs and decomposition of oxidized SWNTs upon ultrasonic irradiation.

## Conclusions

In this study, we examined the influence of sonication during the preparation of SWNT suspensions on the optical properties of SWNTs. When the concentration of SWNTs is high and the treatment time is short, well dispersed SWNTs that maintain their intrinsic optical properties were obtained by sonication. On the other hand, sonication of low concentration SWNT suspensions for a long duration induced the emergence of new red-shifted PL peaks. Under Ar atmosphere, the reaction rate increased and PL peaks assigned to functionalized (6,4) and (6,5)SWNTs were observed at 1043, 1118, and 1221 nm. In the presence of 1-butanol, strong PL peaks emerged at 1043 and 1118 nm under Ar atmosphere without the emergence of the PL peak at 1221 nm. PL control of SWNTs by chemical functionalization to increase the Stokes shift and PL efficiency has attracted significant attention due to their high potential for practical applications. On the other hand, these results clearly show that when preparing dispersions for the analysis of SWNTs and their adducts, it is important to pay attention to the conditions such as sample concentration, surfactants, time for ultrasonic irradiation, and atmosphere. This simple and convenient method for controlling the NIR PL characteristic of SWNTs should contribute to the fundamental understanding of the nature of SWNTs and their practical application as NIR PL materials.

## Author contributions

YMa designed the study and wrote the initial draft. MY, MS, and YMi assisted in the preparation of the manuscript. YK and AN have contributed to sample preparation, data collection, and interpretation. SO, YMi, and KM have contributed to UCPL experiment and interpretation. JM and MM have contributed to XPS measurement and interpretation. All authors discussed the results and contributed to the manuscript.

## Conflicts of interest

There are no conflicts to declare.

## Acknowledgements

This work was partially supported by KAKENHI (Grant Number JPH1702735, JP15H05408), JST CREST (JPMJCR18I5), the research program “dynamic alliance for open innovation bridging human, environment

and materials” within the “Network Joint Research Center for Materials and Devices,” Asahi Glass Foundation, Research Foundation for Opto-Science and Technology, and the Nakatani Foundation.

## Notes and references

1. S. Iijima and T. Ichihashi, T. Single-Shell Carbon Nanotubes of 1-nm Diameter. *Nature* 1993, **363**, 603–605.
2. D. S. Bethune, C. H. Kiang, M. S. de Vries, G. Gorman, R. Savoy, J. Vazquez and R. Beyers, Cobalt-Catalysed Growth of Carbon Nanotubes with Single-Atomic-Layer Walls. *Nature* 1993, **363**, 605–607.
3. R. Sato, M. Fujita, G. Dresselhaus and M. S. Dresselhaus, Electronic Structure of Chiral Graphene Tubules. *Appl. Phys. Lett.* 1992, **60**, 2204–2206.
4. H. Kataura, Y. Kumazawa, Y. Maniwa, I. Umez, S. Suzuki, Y. Ohtsuka and Y. Achiba, Optical Properties of Single-Wall Carbon Nanotubes. *Syn. Met.* 1999, **103**, 2555–2558.
5. X. Tu, S. Manohar, A. Jagota and M. Zheng, DNA Sequence Motifs for Structure-Specific Recognition and Separation of Carbon Nanotubes. *Nature* 2009, **460**, 250–253.
6. S. M. Bachilo, M. S. Strano, C. Kittrell, R. H. Hauge, R. E. Smalley and R. B. Weisman, Structure-Assigned Optical Spectra of Single-Walled Carbon Nanotubes. *Science* 2002, **298**, 2361–2366.
7. G. Hong, J. C. Lee, J. T. Robinson, U. Raaz, L. Xie, N. F. Huang, J. P. Cooke and H. Dai, Multifunctional in vivo Vascular Imaging using Near-Infrared II Fluorescence. *Nat. Med.* 2012, **18**, 1841–1846.
8. M. S. Hofmann, J. T. Glückert, J. Noé, C. Bourjau, R. Dehmel and A. Högele, Bright, Long-Lived and Coherent Excitons in Carbon Nanotube Quantum Dots. *Nat. Nanotechnol.* 2013, **8**, 502–505.
9. T. Endo, J. Ishi-Hayase and H. Maki, Photon Antibunching in Single-Walled Carbon Nanotubes at Telecommunication Wavelengths and Room Temperature. *Appl. Phys. Lett.* 2015, **106**, 113106.
10. S. Ghosh, S. M. Bachilo, R. A. Simonette, K. M. Beckingham and R. B. Weisman, Oxygen Doping Modifies Near-Infrared Band Gaps in Fluorescent Single-Walled Carbon Nanotubes. *Science* 2010, **330**, 1656–1659.
11. Y. Maeda, J. Higo, Y. Amagai, J. Matsui, K. Ohkubo, Y. Yoshigoe, M. Hashimoto, K. Eguchi, M. Yamada, T. Hasegawa, Y. Sato, J. Zhou, J. Lu, T. Miyashita, S. Fukuzumi, T. Murakami, K. Tohji, S. Nagase, T. Akasaka, Helicity-Selective Photoreaction of Single-Walled Carbon Nanotubes with Organosulfur Compounds in the Presence of Oxygen. *J. Am. Chem. Soc.* 2013, **135**, 6356–6362.
12. Y. Zhang, N. Valley, A. H. Brozena, Y. Piao, X. Song, G. C. Schatz and Y. Wang, Propagative Sidewall Alkylcarboxylation that Induces Red-Shifted Near-IR Photoluminescence in Single-Walled Carbon Nanotubes. *J. Phys. Chem. Lett.* 2013, **4**, 826–830.
13. Y. Maeda, Y. Takehana, M. Yamada, M. Suzuki and T. Murakami, Control of the

Photoluminescence Properties of Single-Walled Carbon Nanotubes by Alkylation and Subsequent Thermal Treatment. *Chem. Commun.* 2015, **51**, 13462–13465.

14. Y. Maeda, S. Minami, Y. Takehana, J. S. Dang, S. Aota, K. Matsuda, Y. Miyauchi, M. Yamada, M. Suzuki, R. S. Zhao, X. Zhao and S. Nagase, Tuning of the Photoluminescence and Up-Conversion Photoluminescence Properties of Single-Walled Carbon Nanotubes by Chemical Functionalization. *Nanoscale* 2016, **8**, 16916–16921.

15. T. Shiraki, T. Shiraishi, G. Juhász, and N. Nakashima, Emergence of New Red-Shifted Carbon Nanotube Photoluminescence Based on Proximal Doped-Site Design. *Sci. Rep.* 2016, **6**, 28393.

16. Y. Maeda, Y. Konno, M. Yamada, P. Zhao, X. Zhao, M. Ehara and S. Nagase, Control of Near Infrared Photoluminescence Properties of Single-Walled Carbon Nanotubes by Functionalization with Dendrons. *Nanoscale* 2018, **10**, 23012–23017.

17. X. Wu, M. Kim, H. Kwon and Y. Wang, Photochemical Creation of Fluorescent Quantum Defects in Semiconducting Carbon Nanotube Hosts. *Angew. Chem. Int. Ed.* 2018, **57**, 648–653.

18. H. Kwon, A. Furmanchuk, M. Kim, B. Meany, Y. Guo, G. C. Schatz and Y. Wang, Molecularly Tunable Fluorescent Quantum Defects. *J. Am. Chem. Soc.* 2016, **138**, 6878–6885.

19. Y. Miyauchi, M. Iwamura, S. Mouri, T. Kawazoe, M. Ohtsu and K. Matsuda, Brightening of Excitons in Carbon Nanotubes on Dimensionality Modification. *Nat. Photon.* 2013, **7**, 715–719.

20. Y. Maeda, E. Sone, A. Nishino, Y. Amagai, W. W. Wang, M. Yamada, M. Suzuki, J. Matsui, M. Mitsuishi, T. Okazaki and S. Nagase, Thermal Stability of Oxidized Single-Walled Carbon Nanotubes: Competitive Elimination and Decomposition Reaction Depending on the Degree of Functionalization. *Chem. Eur. J.* 2016, **22**, 15373–15379.

21. Y. Maeda, Y. Takehana, J. S. Dang, M. Suzuki, M. Yamada and S. Nagase, Effect of Substituents and Initial Degree of Functionalization of Alkylated Single-Walled Carbon Nanotubes on Their Thermal Stability and Photoluminescence Properties. *Chem. Eur. J.* 2017, **23**, 1789–1794.

22. M. J. O'Connell, S. H. Bachilo, C. B. Huffman, V. C. Moore, M. S. Strano, E. H. Haroz, K. L. Rialon, P. J. Boul, W. H. Noon, C. Kittrell, J. Ma, R. H. Hauge, R. B. Weisman R. E. Smalley, Band Gap Fluorescence from Individual Single-Walled Carbon Nanotubes. *Science* 2002, **297**, 593–596.

23. K. R. Moonosawmy and P. Kruse, P. To Dope or Not To Dope: The Effect of Sonication Single-Wall Carbon Nanotubes in Common Laboratory Solvents on Their Electronic Structure. *J. Am. Chem. Soc.* 2008, **130**, 13417–13424.

24. S. Mouri, Y. Miyauchi and K. Matsuda, Dispersion-Process Effects on the Photoluminescence Quantum Yields of Single-Walled Carbon Nanotubes Dispersed using Aromatic Polymers. *J. Phys. Chem. C* 2012, **116**, 10282–10286.

25. F. Hennrich, R. Krupke, K. Arnold, J. A. R. Stütz, S. Lebedkin, T. Koch, T. Schimmel and M. M. Kappes, The Mechanism of Cavitation-Induced Scission of Single-Walled Carbon Nanotubes. *J. Phys. Chem. B* 2007, **111**, 1932–1937.



26. J. Z. Sostaric and P. Riesz, Sonochemistry of Surfactants in Aqueous Solutions: An ESR Spin-Trapping Study. *J. Am. Chem. Soc.* 2001, **123**, 11010–11019.
27. M. Ashokkumar, T. Niblett, L. Tantonco and F. Grieser, Sonochemical Degradation of Sodium Dodecylbenzene Sulfonate in Aqueous Solutions. *Aust. J. Chem.* 2003, **56**, 1045–1049.
28. E. Manousaki, E. Psillakis, N. Kalogerakis and D. Mantzavinos, Degradation of Sodium Dodecylbenzene Sulfonate in Water by Ultrasonic Irradiation. *Water Res.* 2004, **38**, 3751–3759.
29. D. Tasis, N. Tagmatarchis, A. Bianco and M. Prato, Chemistry of Carbon Nanotubes. *Chem. Rev.* 2006, **106**, 1105–1136.
30. N. Karousis, N. Tagmatarchis and D. Tasis, Current Progress on the Chemical Modification of Carbon Nanotubes. *Chem. Rev.* 2010, **110**, 5366–5397.
31. Y. Tan and D. E. Resasco, Dispersion of Single-Walled Carbon Nanotubes of Narrow Diameter Distribution. *J. Phys. Chem. B* 2005, **109**, 14454–14460.
32. N. T. Alvarez, C. Kittrell, H. K. Schmidt, R. H. Hauge, P. S. Engel, and J. M. Tour, Selective Photochemical Functionalization of Surfactant-Dispersed Single Wall Carbon Nanotubes in Water. *J. Am. Chem. Soc.* 2008, **130**, 14227–14233.
33. X. Wei, T. Tanaka, N. Akizuki, Y. Miyauchi, K. Matsuda, M. Ohfuchi and H. Kataura, H. Single-Chirality Separation and Optical Properties of (5,4) Single-Wall Carbon Nanotubes. *J. Phys. Chem. C* 2016, **120**, 10705–10710.
34. D. Drijvers, R. De baets, A. De Visscher and H. Van Langenhove, Sonolysis of Trichloroethylene in Aqueous Solution: Volatile Organic Intermediates. *Ultrasonic Sonochem.* 1996, **3**, S83–S90.
35. D. G. Wayment and D. J. Casadonte Jr., Frequency Effect on the Sonochemical Remediation of Alachlor. *Ultrasonic Sonochem.* 2002, **9**, 251–257.
36. Y. Maeda, K. Kuroda, H. Tambo, H. Murakoshi, Y. Konno, M. Yamada, P. Zhao, X. Zhao, S. Nagase and M. Ehara, M. Influence of Local Strain Caused by Cycloaddition on the Band Gap Control of Functionalized Single-Walled Carbon Nanotubes. *RSC Adv.* 2019, **9**, 13998–14003.
37. Y. Maeda, H. Murakoshi, H. Tambo, P. Zhao, K. Kuroda, M. Yamada, X. Zhao, S. Nagase and M. Ehara, Thermodynamic Control of Quantum Defects on Single-Walled Carbon Nanotubes. *Chem. Commun.* 2019, **55**, 13757–13760.
38. Y. Iizumi, M. Yudasaka, J. Kim, H. Sakakita, T. Takeuchi and T. Okazaki, Oxygen-Doped Carbon Nanotubes for Near-Infrared Fluorescent Labels and Imaging Probes. *Sci. Rep.* 2018, **8**, 6272.
39. N. Akizuki, S. Aota, S. Mouri, K. Matsuda and Y. Miyauchi, Efficient Near-Infrared Up-Conversion Photoluminescence in Carbon Nanotubes. *Nat. Commun.* 2015, **6**, 8920.
40. D. Ogrin, J. Chattopadhyay, A. K. Sadana, W. E. Billups and A. R. Barron, Epoxidation and Deoxygenation of Single-Walled Carbon Nanotubes: Quantification of Epoxide Defects. *J. Am. Chem. Soc.* 2006, **128**, 11322–11323.
41. C. Annese, L. D'Accolti, G. Giambastiani, A. Mangone, A. Milella, G. Tuci and C. Fusco,

Tunable Epoxidation of Single-walled Carbon Nanotubes by Isolated Methyl(trifluoromethyl)dioxirane.  
*Eur. J. Org. Chem.* 2014, **8**, 1666–1671.